

# EFFECT OF PREPARATION TEMPERATURE ON ETHYLCELLULOSE MICROSPHERE PROPERTIES PREPARED BY OIL-IN-OIL EMULSION SOLVENT EVAPORATION PROCESS

Prasanta K. Mohapatra<sup>a\*</sup> and Sunit K. Sahoo<sup>b</sup>

(Received 19 April 2020) (Accepted 10 October 2022)

## ABSTRACT

The present study aims to formulate ethylcellulose microspheres using the oil-in-oil emulsion solvent evaporation method and judge the outcome of processing temperature on their features. The effects of the evaporation rate of the solvent on the particle properties and drug release characteristics of the microspheres were studied. Here, microspheres were prepared at different processing temperatures, viz., 10 °C, 25 °C, and 40 °C, and their impact on the various characteristics of microspheres like surface topography, micrometrics, yield percent, encapsulation efficiency, *in vitro* dissolution, Fourier-transform infrared spectroscopy (FTIR) and release kinetics were elaborately studied. The FTIR study revealed that processing temperature did not affect drug-polymer compatibility. The study observed that the processing temperature had a great influence on the various characteristics of the prepared microsphere. It was observed from sieve analysis that the mean particle size of the microsphere increased with an increase in processing temperature, and the SEM study also corroborated the same result. SEM photographs showed processing at a higher temperature resulted in particles with a smooth surface, in contrast to a lower processing temperature that forms a bumpy surface. Furthermore, a higher temperature favoured formulation with a higher entrapment efficiency ( $94.42 \pm 0.9 \%$ ) as compared to a lower temperature ( $85.2 \pm 0.72 \%$ ). For a noteworthy timeframe, indinavir sulfate forms a solid solution in the ethylcellulose matrix and proceeds with the amorphous state. The results of an *in vitro* drug dissolution study showed that microspheres formulated at a higher temperature had a more sustaining effect as compared to those formulated at a lower temperature, which may have resulted due to their higher mean particle size. Using the Korsmeyer Peppas power law, it was found that the way drugs are released is controlled by diffusion.

**Keywords:** Microspheres, solvent evaporation, preparation temperature, scanning electron microscope, release kinetics

## ABBREVIATIONS

kV: kilovolt; mA: milliampere; DR: drug release  
3D: three Dimensional; KBr: Potassium bromide; r<sub>2</sub>:  
Correlation Coefficient K: the rate constant; n: release  
exponent; ASTM: American Society for Testing and  
Materials; Vs: Versus; cm<sup>-1</sup>: Wavelengths per unit distance/  
typically centimeters

## INTRODUCTION

Different formulations are chosen for different drugs due to their physicochemical properties. In pharmacy, the long-term release of low-molecular-weight, thermally

unstable, and water-soluble medications is a hot topic<sup>1,2</sup>. Microspheres are usually used to wrap water-soluble pharmaceuticals for long-term release because the drugs are spread out in the skeleton of water-insoluble materials<sup>3,4</sup>. Moreover, the stability and release kinetics of microspheres may be affected by different microsphere production processes<sup>5</sup>. Spray-drying is a viable and cost-effective approach for fabricating microspheres, and it is frequently utilized in pharmaceutical manufacturing<sup>6,7</sup>. However, because the solvent was volatilized at a high temperature during the manufacture, it is not suited for thermally unstable pharmaceuticals because the drugs may break down. The solvent evaporation technique is extensively used to avoid high temperatures since it may be carried out at a moderate temperature<sup>8</sup>. Typically, emulsions based on oil-in-water (O/W) emulsification are generated, and the internal oil phase is evaporated to

<sup>a</sup> Moradabad Educational Trust Group of Institutions Faculty of Pharmacy, Moradabad -244 001, Uttar Pradesh, India

<sup>b</sup> Pharmaceutics Division, University Department of Pharmaceutical Sciences, Utkal University, Bhubaneswar -751 004, Odisha, India

\*For Correspondence: E-mail: mahapatra.kjr@gmail.com

<https://doi.org/10.53879/id.60.05.12481>

precipitate the polymer material, resulting in microspheres, as previously reported<sup>9,10</sup>. However, because the drug diffuses into the external aqueous phase, this approach may cause low drug loading efficiency, especially for those medicines with low molecular weight and good water solubility. Furthermore, the microspheres obtained may have rapid drug release. Oil-in-oil (O/O) emulsions can be created by substituting organic solvents for the exterior aqueous phase in the solvent evaporation technique. Because the drug is soluble in the external oil phase, this could increase encapsulation effectiveness and drug release behavior<sup>8</sup>. Based on the current number of studies being done by experts from all over the world, it is clear that microsphere release rates are affected by a lot of different things. The quality of the microspheres created is heavily influenced by the processing parameters utilized during preparation, in addition to the type of polymer used. The release of a drug from the system is influenced by properties such as size and density, matrix structure, which includes the surface and internal areas, drug encapsulation efficiency, and drug distribution. As a result, scientists have been investigating the many preparation circumstances that could affect the above properties<sup>11</sup>. Several articles have looked at how solvent removal techniques affect poly-(DL-lactide-co-glycolide) (PLGA) microspheres. The way and speed of solvent removal, such as the temperature gradient and the dilution of the continuous phase methods, affected how the microspheres were made on the inside<sup>11</sup>.

In recent years, the preparation of polymeric microspheres has been widely reported using a microencapsulation technique based on the emulsification solvent evaporation process. One of the main problems with the solvent evaporation method is that it can take a long time to remove the solvent. This can take up to several hours. As a result, many academics have investigated ways to shorten the time it takes for the solvent to evaporate. Although increasing the temperature reduced the required preparation time, there were several drawbacks: the total weight recovered fell; the size distribution changed toward the bigger size; drug loading efficiency declined, and the morphology became rougher. As a result of the uncontrollable acceleration of the solvent evaporation rate, the quality of the microspheres for controlled drug release has deteriorated<sup>12</sup>. In the manufacture of PLLA or PDLLA microspheres loaded with hydrophobic active ingredients such as progesterone and lidocaine, dichloromethane solution (DCM) and polyvinyl alcohol solution (PVA) have commonly been used as a solvent and stabilizing agent of the suspension, respectively<sup>14</sup>. The microencapsulation by solvent evaporation strategy in microsphere planning is a difficult procedure that can be

influenced by a variety of procedure parameters, such as the solvent evaporation rate<sup>13,14</sup>, temperature<sup>15-17</sup>, polymer solubility, emulsion phase of drug and excipients<sup>18,19,20</sup>, dispersion stirring rates<sup>20-22</sup>, porosity, solubility, viscosity, surfactant amount, the volume of inner and outer phases and volume ratio<sup>23-25</sup> drug<sup>24,26</sup>. The delivery of active ingredients such as narcotic antagonists, local anesthetics, steroid hormones, anticancer drugs, and other peptides has already been thoroughly investigated using microspheres, which are composed of a drug dispersed in a spherical polymer matrix. The oil-in-water emulsion-solvent evaporation method was used to integrate nifedipine, a calcium-channel blocking drug, into poly (DL-lactide-co-glycolide) microspheres<sup>24</sup>. The temperature at which the microspheres were prepared had an impact on their formulation and properties. Some authors have previously focused on and reported on the microsphere's base diameter and size distribution breadth<sup>11,15,18</sup>, particle shape<sup>13,15</sup>, porosity<sup>11</sup> and drug loading<sup>11</sup>. There are many advanced fields where polymer microspheres have been used because they have a lot of surface area and can be recycled easily. They also cost less than other materials and can be reused. According to the presence or absence of networked structures, polymer microspheres can be classified as linear microspheres or crosslinked microspheres; they can also be split into hydrophilic and hydrophobic polymer microspheres based on their affinity for water. Hydrophobic linear polymer microspheres are the focus of current research<sup>27</sup>.

The size of the microsphere, encapsulation effectiveness, and rate of drug release are all influenced by the polymeric membrane. In matrix or coating systems, ethylcellulose was used as a non-swellable, insoluble component. When ethylcellulose is employed as a polymer, it generates microcapsules that are stable, pH-independent, and have a long release time<sup>28</sup>. The manufacturing of microcapsules was completed in this article by using solvent evaporation to solidify the emulsion. The microdroplets, also called the emulsion phase, are a mixture of an organic solvent and a polymeric material that is used to encapsulate the medicament. The quaternary ammonium product, which is used as a virucide<sup>21</sup>, is encapsulated. There was only one report instituted here, in which the influence of temperature on microspheres was studied using a polymer (ethylcellulose). In this way, the goal of this investigation was to see how the impact of preparation temperature on ethylcellulose microspheres and their properties differed depending on the temperature. The microspheres were manufactured at three different temperatures: low, room and high, where more apparent impacts were expected. particle size, morphology, drug

dissolution study, and release kinetics were all used to look at the microspheres that were made.

## MATERIALS AND METHODS

### Materials

Cipla, Ltd., Mumbai, India, provided indinavir sulfate as a gift. CDH Pvt. Ltd. in New Delhi, India, supplied paraffin liquid light and ethylcellulose. SD Fine Chem. Ltd, Mumbai, India, provided Span 80. All the other chemicals obtained from the authorized dealer were analytical grade<sup>9,29</sup>.

### Methods

#### Experimental design

Factorial design is one method for studying the impact of a factor on the quality-determining parameters of any formulation. Under the direction of a plan of examinations, this structure was employed to investigate the impact of autonomous elements. An experimental design is employed in this study to optimize the preparation temperatures and mean particle size, which are specified as factors  $X_1$  and  $X_2$  and learned at three levels each. The number of experiments necessary for this study is determined by the number of independent variables used. Each study used the % of entrapment efficiency ( $Y_1$ ) and the percent total drug release (TDR) after 4 h of indinavir sulfate ( $Y_2$ ). Table I shows the variables, with  $X_1$  having the most impact.  $X_2$  the average result of altering one element at a time from a low to a high number. The reaction is described by the expression " $X_1X_2$ " when two elements change at the same time<sup>29,30,31</sup>.

#### Microsphere preparation

The microspheres were made in a liquid paraffin solvent system and emulsified using a solvent evaporation emulsification process. The rate of increase in temperature of the water bath was used to control the pace of solvent evaporation. Using a magnetic stirrer at 500 rpm, ethylcellulose (1500 mg) and indinavir sulfate (500 mg) were dissolved in an acetone-methanol mixture (10:1 ratio) for about 5 min (Remi Equipments, Model 2MIH). The resultant dispersion was placed into a 250 mL beaker containing 100 mL liquid paraffin light and 2 % Span 80 mixture while being put forward at constant temperatures of 10 °C, 25 °C, and 40 °C. Initially, a disc blade [4 cm in diameter] with a mechanical stirrer (Remi Motors, Model No.RO-123R, Mumbai) was used and rotated at 750 rpm, and the formulation of microspheres was continued at temperatures (10 °C, 25 °C, and 40 °C) for 4 to 5 h until complete evaporation of acetone and methanol was achieved. Each formulation was rinsed with cyclohexane

after the microspheres were filtered using Whatman No. 1 filter paper, and then it was dried at room temperature for 24 h. Microspheres were produced in triplicate for each of the different temperature ranges. Except where otherwise stated, all microsphere characterization studies were conducted using one-day-old samples<sup>32-35</sup>.

#### Particle size analysis

The size of the microspheres was evaluated using conventional ASTM sieves [American Society for Testing and Materials]. A sieve set was used with sieve apertures of [1000 µm, 710 µm, 500 µm, 355 µm, 250 µm, and 180 µm] and a nest of sieves ranging from # 16 to # 80 mesh. A mechanical sieve shaker was used to sift the samples for 20 min each time (Cuprit Electrical Co. India). The particles kept on each sieve were weighed at this point, and the % held on each sieve was calculated. A histogram of the % weight held against the particle was plotted, and the mechanical sieve shaker was used to sift the particles for 20 min. The particles held on each sieve were weighed at this point, and the percentage held on each sieve was calculated. The % weight held against the particle is shown as a histogram (Fig. 2)<sup>36-39</sup>.

#### Yield % of microspheres

After drying in a hot air oven, the prepared microspheres were weighed. The total theoretical mass of all the components used in the microsphere formulation was divided by the mass of the obtained microspheres in that batch and multiplied by 100.

$$\text{Yield \%} = \frac{\text{Weight of obtained microspheres (g)}}{\text{Theoretical weight of the microspheres (g)}} * 100 \quad \dots(1)$$

#### Drug encapsulation efficiency

By extracting it in triple-distilled water, the concentration of indinavir sulfate in the microspheres was measured. 50 mg crushed and powdered microspheres were combined with 2 mL acetone, extracted with 50 mL triple distilled water, and agitated for 24 h on a mechanical shaker. The solution was separated using Whatman No.1 filter paper, and the amount of indinavir sulfate was quantified by utilizing a UV-Visible spectrophotometer at 259 nm [Elico, SL159] following appropriate dilutions. From the measured optical density data, the drug content and entrapment efficiency were determined (Table III)<sup>42-44</sup>.

$$\text{Drug entrapment efficiency (\%)} = \frac{\text{Experimental drug content}}{\text{Theoretical drug content}} * 100 \quad \dots(2)$$

**Table I: Formulation characteristics of experimental design layouts**

Independent variables		Dependent variables	
X1	X2	Y1	Y2
Preparation temperature	Mean particle size	Entrapment efficiency (%)	% TDR at 4 h
Coded levels			
Low level	Middle level		High level
-1	0		+1
Preparation temperature			
10 °C	25 °C		40 °C
Mean particle size			
266	423		518

**Table II: Summary of results of regression analysis, formulation**

Drug entrapment efficiency (%)							
Response ( $Y_1$ )	$\beta_0$	$\beta_1$	$\beta_2$	$\beta_{12}$	$\beta_{11}$	$\beta_{22}$	R <sup>2</sup> value
Coefficient	+89.8303	+2.31857	+2.305	-0.166687	-0.226667	+0.3575	0.9998
P Value	< 0.0001	< 0.0001	< 0.0001	+0.0177	+0.0203	+0.0070	
TDR After 4 h (%)							
Response ( $Y_2$ )	$\beta_0$	$\beta_1$	$\beta_2$	$\beta_{12}$	$\beta_{11}$	$\beta_{22}$	R <sup>2</sup> value
Coefficient	+81.6275	-7.90024	-8	-1.22564	-1.66667	-3.84971	0.9990
P Value	+0.0001	< 0.0001	< 0.0001	+0.0177	+0.0203	+0.0023	

**Table III: Physical characteristics of the microspheres**

Formulation code	Mean particle size ( $\mu\text{m}$ )*	Bulk density ( $\text{g mL}^{-1}$ )*	Tapped density ( $\text{g mL}^{-1}$ )*	Yield (%) *	Entrapment efficiency (%) *	Carr's index*	Packing factor*
F1	266.86 $\pm$ 4.5	0.48 $\pm$ 0.06	0.69 $\pm$ 0.04	97.15 $\pm$ 2.35	85.2 $\pm$ 0.72	30 $\pm$ 0.8	1.42 $\pm$ 0.05
F2	423.30 $\pm$ 5.3	0.47 $\pm$ 0.05	0.52 $\pm$ 0.03	95.10 $\pm$ 1.86	90.49 $\pm$ 1.02	10 $\pm$ 0.6	1.11 $\pm$ 0.04
F3	518.34 $\pm$ 7.2	0.47 $\pm$ 0.03	0.50 $\pm$ 0.04	90.95 $\pm$ 1.58	94.42 $\pm$ 0.9	5.2 $\pm$ 0.9	1.05 $\pm$ 0.07

\*Mean of triplicate data specified ( $n=3 \pm SD$ )

**Table IV: Various parameters of the model equations of the *in vitro* release kinetics**

Formulation code	Zero order	First order	Higuchi	Hixon Crowell	Korsemeier-Peppas	Release exponent	Best fit model
	r <sup>2</sup>					n	
F1	0.995	0.976	0.990	0.991	0.984	0.446	Zero order
F2	0.995	0.955	0.995	0.982	0.994	0.381	Zero order
F3	0.995	0.900	0.971	0.949	0.965	0.345	Zero order

( $r^2$  = correlation coefficient,  $n$  = release exponent)

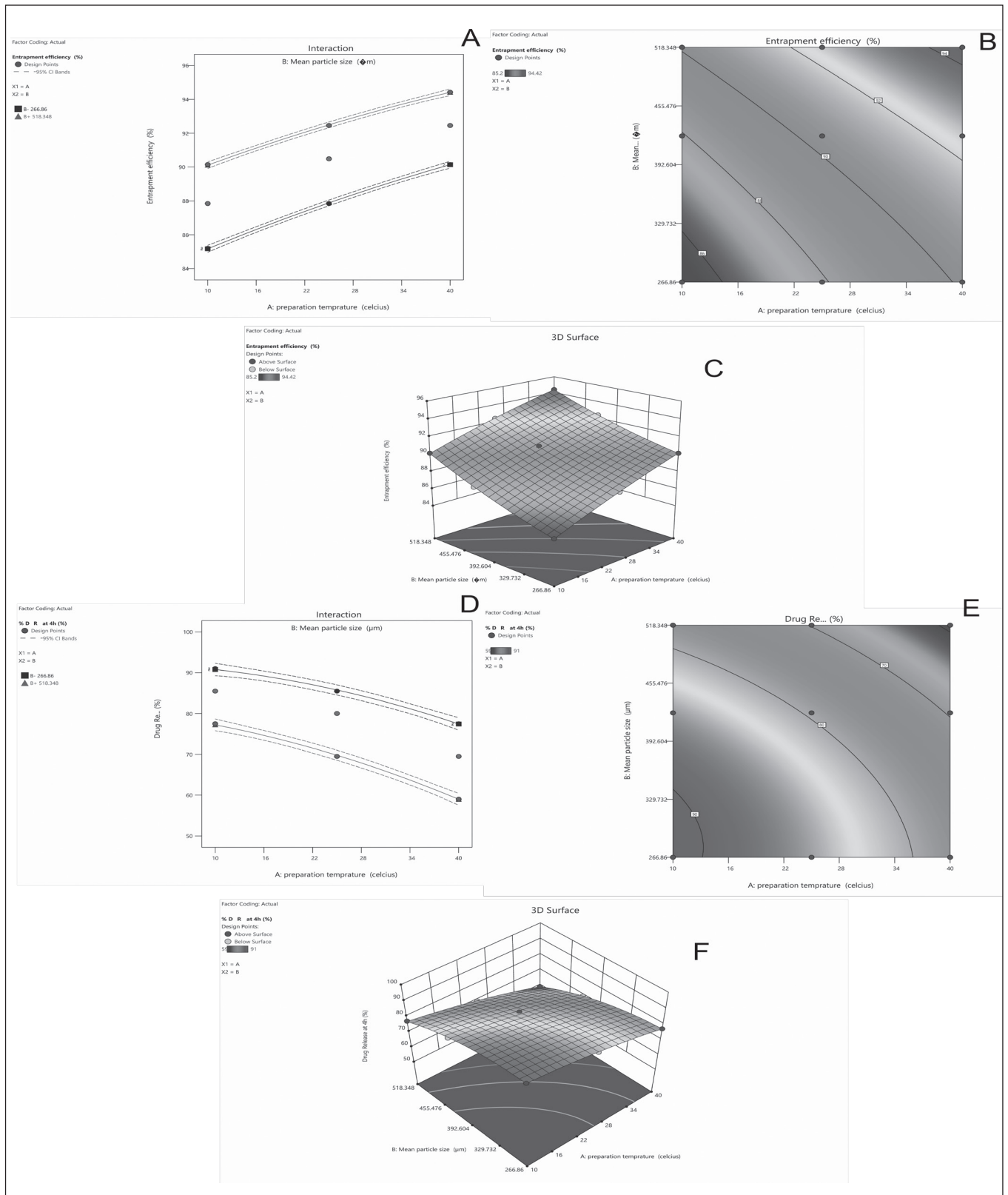


**Fig. 1: Interaction and contour response surface plot and 3D graph display the influence of different preparation temperatures and mean particle size ( $\mu\text{m}$ ) on entrapment efficiency (%) (A, B & C) and % DR after 4 h (D, E & F) mean of triplicate data specified ( $n = 3 \pm \text{SD}$ )**



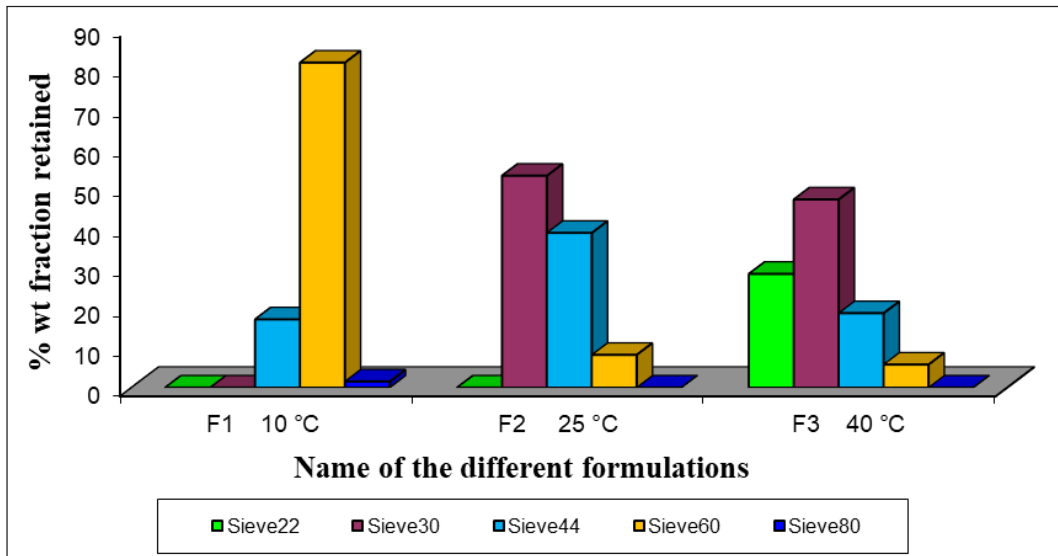


Fig. 2: Percentage of weight retained mean of triplicate data specified (n= 3 ± SD)

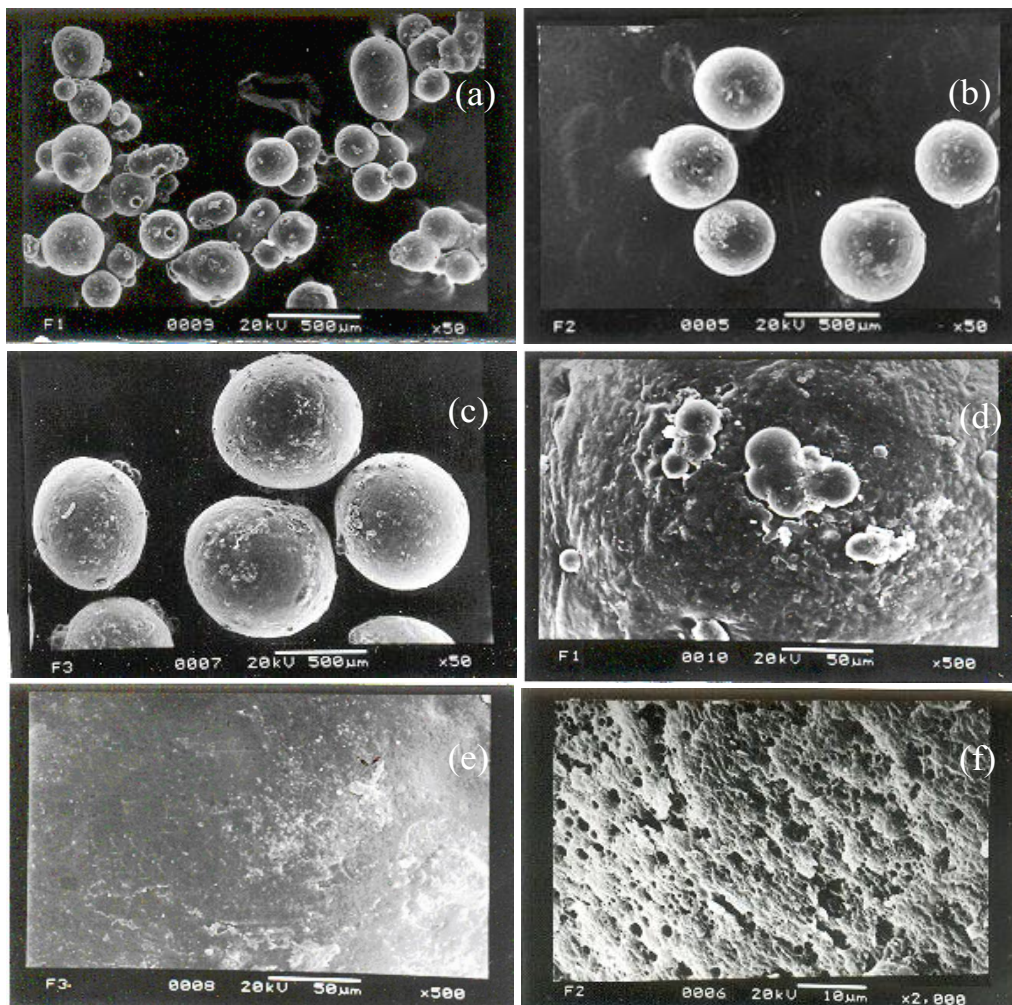
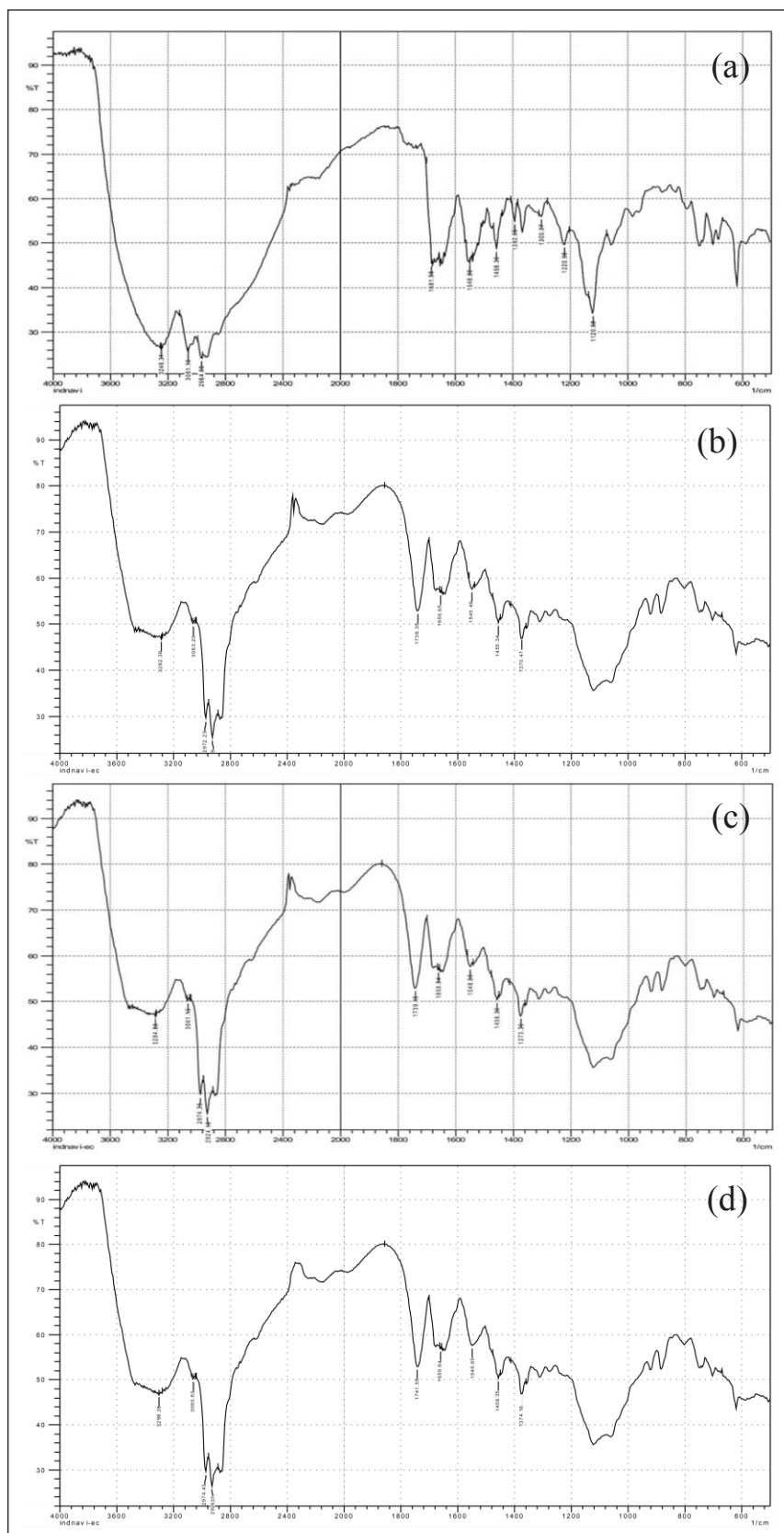


Fig. 3: SEM before dissolution, photographs of microspheres were obtained at temperatures of, a-10 °C, b-25 °C, c-40 °C at 50x magnification, and d-10 °C, e-40 °C at 500x magnification and after dissolution f-25 °C at 2000x magnification



**Fig. 4: FTIR spectra of drug indinavir sulfate (a) and ethylcellulose microspheres at 10 °C, 25 °C, and 40 °C (b), (c) & (d) scanned from 4000  $\text{cm}^{-1}$  to 400  $\text{cm}^{-1}$  at the resolution 2  $\text{cm}^{-1}$**

### Scanning electron microscopy

A scanning electron microscope (SEM) (JEOL JSM 5200) was used to figure out the shape and surface parameters of microspheres. Before the investigation, the microspheres were positioned on the metallic support with a thin, sticky tape, and the samples were carbon-coated and sputtered with gold [Fine coat, ion sputter JFC-1110] under vacuum to make them electron conductive, and 14 kV was the accelerating voltage. Photomicrographs of drug-loaded microspheres before and after dissolution were taken (Fig. 3)<sup>45-48</sup>.

### Fourier Transform Infrared Spectrometry studies

Fourier transform infrared spectroscopy (FTIR) JASIO [Model No.410] was used to record the spectra of whole drug and drug-loaded microspheres. The produced samples [2 mg sample in 200 mg KBr] were held open using KBr discs. Indinavir sulfate, pure drug, and ethylcellulose microspheres were scanned in an FTIR spectrophotometer from 4000  $\text{cm}^{-1}$  to 400  $\text{cm}^{-1}$  with a resolution of 2  $\text{cm}^{-1}$  and evaluated for any shifts in functional peaks<sup>49-51</sup>.

### Indinavir sulfate release studies

The indinavir sulfate release kinetics were determined using the United States Pharmacopeia (USP) dissolving mechanical assembly (LAB INDIA, DISSO-2000, Mumbai, India) under sink conditions. Microspheres (100 mg) were precisely weighed and distributed in triple distilled water before being swirled at 100 rpm at 37 °C for up to 100 percent DR. The whole DR, samples were obtained at 30, 60, 90, 120, 150, 180, and 210 min, and the concentration of indinavir sulfate was measured spectrophotometrically at 259 nm. Using a regression equation of the calibration curve, the concentration

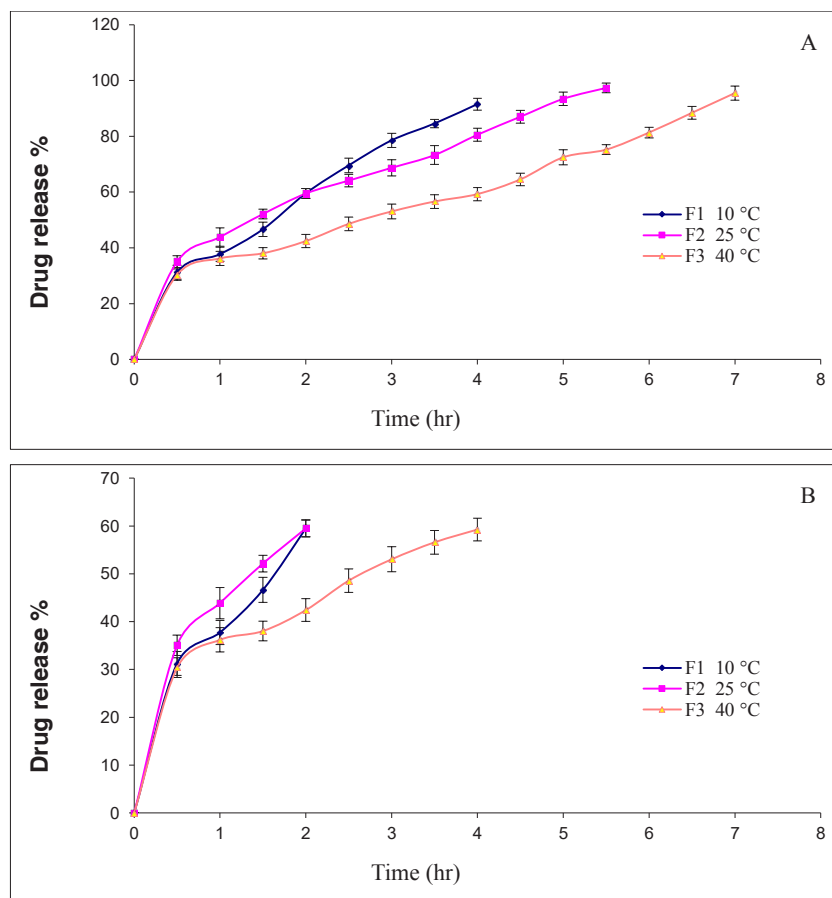


**Fig. 5: Microsphere release profile *in vitro* at various temperatures (a), and drug release up to 60% (b)**

of indinavir sulfate in test samples was adjusted and estimated<sup>52-55</sup>.

### Release kinetics studies

Different kinetic models, such as Korsmeyer-Peppas, Higuchi, and Hixon Crowell, first and zero-order, were used to investigate drug kinetics release. Data from *in vitro* DR measurements were put into different kinetic models to assess the release kinetics. Higuchi's model as a total % of drug discharged vs time in square root, first-order as a log total % of drug remaining vs time, and zero-order as a total % of drug discharged vs time. The assessment of the correlation coefficient, which was close to '1', confirmed the best-fit model<sup>41</sup>. The data was introduced to find the best model. The mechanism of release pursues "Fickian diffusion" if "n" for (sphere) is 0.43 or less, and upper estimates of 0.43-0.85 for mass transport follow a non-Fickian (anomalous transport) model. If the 'n' value is 0.85, case II transport and DR will follow the Higuchi model. The mechanism of DR is seen as super case II transport for estimates of 'n' greater than 0.85<sup>56,57</sup>.

## RESULTS

### Experimental design

From the 3D graph, it was concluded that as the preparation temperatures declined from 40 °C to 10 °C, the mean particle size diminished, and due to the creation of small particles, the entrapment efficiency also diminished. The following is the polynomial equation for factorial designs.

$$Y = \beta_0 + \beta_1 X_1 + \beta_2 X_2 + \beta_{12} X_1 X_2 + \beta_{11} X_1^2 + \beta_{22} X_2^2 \quad (3)$$

The phrase " $X_1 X_2$ " describes how the reaction varies when both elements change at the same time. Each trial's response (Y) is measured as a dependent variable, and the % of entrapment efficiency ( $Y_1$ ) and the % of TDR at 4 'h' ( $Y_2$ ) were used. After evaluating the amount of the coefficient and the mathematical sign it bears, the polynomial equations can be employed to conclude (i.e., positive, or negative). The Design of Expert version 13 was used to examine the data. The  $R^2$  values of 0.9998, and 0.9990 for the % of entrapment efficiency ( $Y_1$ ) and the % of TDR at 4 'h' ( $Y_2$ ), respectively, indicate a high connection between dependent and

independent variables. Because the response variables were significant ( $p < 0.05$ ), there was no need to create reduced models. The terms having a P value of less than 0.05 were judged statistically significant and kept in the entire model. According to the results of ANOVA (Table II), the F values for % of entrapment effectiveness ( $Y_1$ ) and % of TDR after 4 'h' of indinavir sulfate ( $Y_2$ ) were 2546.49 and 577.21, respectively. For all dependent variables, calculated F values were larger than tabulated, indicating that the factors chosen had substantial effects. Multiple regression analysis revealed that both covariates had a statistically significant impact on all dependent variables, with a  $p < 0.05$  significance level.

### Full model for the % entrapment efficiency

Fig. 1a, 1b, and 1c show the interaction, contour plot, and response surface plot for the % of entrapment efficiency, revealing that an increase in the % of entrapment efficiency was found with increasing preparation temperature ( $X_1$ ) and mean particle size ( $X_2$ ). There was no evidence of interaction or nonlinearity. The significant



levels of coefficient  $\beta_0, \beta_1, \beta_2, \beta_{12}, \beta_{11},$  and  $\beta_{22}$  had a P-value less than 0.0500 for the % of entrapment efficiency. At  $p < 0.05$ , the coefficient was judged to be significant. The following was the model for the % of entrapment efficiency:

$$\text{Entrapment efficiency} = 89.8303 + 2.31857 * X_1 + 2.305 * X_2 + -0.166687 * X_1 X_2 + -0.226667 * X_1^2 + 0.3575 * X_2^2 \quad (4)$$

### Full model for % TDR at 4 h

The interaction, contour plot, and response surface plot for % TDR after 4 h ( $Y_2$ ) are shown in Fig. 1d, 1e, and 1f, respectively, and demonstrate that a rising preparation temperature ( $X_1$ ) and mean particle size ( $X_2$ ) resulted in a commensurate decrease in the % TDR rate of microspheres. There was no evidence of interaction or nonlinearity. The significant levels of coefficient  $\beta_0, \beta_1, \beta_2, \beta_{12}, \beta_{11},$  and  $\beta_{22}$  had a P-value less than 0.0500 for the % of TDR after 4 'h'. At  $P < 0.05$ , the coefficient was judged to be significant. The following was the model for % TDR after 4 h:

$$\text{TDR \% at 4 'h'} = 81.6275 + -7.90024 * X_1 + -8 * X_2 + -1.22564 * X_1 X_2 + -1.66667 * X_1^2 + -3.84971 * X_2^2 \quad (5)$$

### Particle size determination

Each batch of microspheres was subjected to sieve analysis. Table II and Fig. 2, summarize the results, indicating that preparation temperature has a significant impact on microparticle size. Microspheres with a larger average molecule size and a wider molecule size distribution are generated when a higher planning temperature is linked. After both emulsion phases (oil and organic) have been emulsified, the inner solvent diffuses into the outer, and the solvent evaporates from the system through the outer oil phase. Higher preparation temperatures reduce viscosity and raise the total permeability coefficient of the inner phase solvent, increasing the charge per unit of solvent removal. At higher temperatures, emulsion droplets harden faster. They may not "have time" to be influenced by stirrer shear forces, which lean to minimize droplets.

### Drug encapsulation and yield %

All batches of microspheres were examined for drug encapsulation efficiency. The encapsulation efficiencies for F1, F2, and F3 were found to be 85.2%, 90.49 %, and 94.42 %, respectively. The disparity in encapsulation efficiency between batches (Table III) is comprehensible, given the low solubility of indinavir sulfate in liquid paraffin<sup>30</sup>. It was found that the temperature had a moderate effect on the microencapsulation efficiency of indinavir sulfate

microspheres. The yield % of the microspheres F1 and F2 are higher than that of the microsphere F3, implying that the production yield of prepared microspheres at low temperatures is higher than that at high temperatures.

### Scanning electron microscopy

SEM micrographs of microspheres were prepared under different temperature conditions: 10 °C, 25 °C and 40 °C. Some morphological features, e.g., the diameter, the shape of particles, and surface characteristics can be observed (Fig. 3), as comfortably as their dependence on preparation temperature. When temperatures are low, particles don't have a regular spherical shape, but as temperatures increase, they start to take on a more spherical shape (Fig. 3a & 3b). Surface properties alter together with the temperature increase. Particles formed at 10 °C have a bumpy, wrinkled surface that is adhered to by smaller slightly irregular particles (Fig. 3a). With expanding temperature, the surface moves toward becoming smoother and expanded in size and the particles more circular (Fig. 3d & 3e).

### Fourier Transform Infrared Spectrometry

The FTIR spectra demonstrates that there is no substantial difference between pure medicament (indinavir sulfate) and microspheres when utilizing FTIR spectroscopy at 10 °C, 25 °C, and 40 °C (Fig. 4). The qualities of unpolluted drug prominent peaks at 3246.31  $\text{cm}^{-1}$ , 3051.13  $\text{cm}^{-1}$ , 2960.26  $\text{cm}^{-1}$ , 1681.98  $\text{cm}^{-1}$ , 1548.89  $\text{cm}^{-1}$ , 1496.30  $\text{cm}^{-1}$ , 1392.65  $\text{cm}^{-1}$ , 1300.07  $\text{cm}^{-1}$ , 1220.98  $\text{cm}^{-1}$ , and 1120.63  $\text{cm}^{-1}$  corresponding to OH stretching, NH stretching of secondary amine, C–H stretching (–C≡CH), C–H stretching ( $\text{CH}_3$ ), C–H stretching (asymmetric), C–H stretching (symmetric) and C=O stretching stayed unaltered contrasted with microspheres. It was concluded that there was a compatibility between the medicament and the polymer.

### Drug release behavior

The mean particle diameter and distribution breadth, the porosity of the particles, and the homogeneity of medicament spreading inside microparticles all influence the DR from microspheres. When *in vitro* DR data from different formulations were looked at, it was seen that formulations made at a higher temperature of 40 °C had a sustained drug release than formulations made at a lower temperature of 10 °C (Fig. 5). The mean particle size of the microspheres was not as large at a lower handling temperature as it was at a higher preparation temperature (Fig. 2). The drug-filled microspheres were released in a sink state in a USP dissolution apparatus (LAB INDIA, DISSO-2000, Mumbai, India) that rotated

at 100 rpm at 37 °C. The collected products were tested using UV-Visible spectroscopy at 259 nm. The global temperature essence, as well as the drug delivery profile, were established. Changes in surface area due to particle surface roughness and porosity result in differences in release profiles. One may argue that particle surface properties are more important than particle size, based on the comparability of dissolution profiles from whole samples and size fractions.

### Release kinetic modeling

To determine the best release model represents the DR model, *in vitro* release data was substituted in many models, such as zero and first-order, Higuchi, Hixon Crowell, and Korsmeyer Peppas's kinetics models. Table IV lists the release profiles that correspond to the model. The highest regression found was the zero-order equation (0.995). The Korsmeyer-Peppas equation for the sphere was used to explain the DR mechanism. The slope (n) estimation was determined and observed to be F2 (0.381) and F3 (0.345), both of which are less than 0.43, indicating Fickian diffusion, and 'n' data of F1 (0.446) which is between 0.34 and 0.85, indicating non-Fickian anomalous transport.

## DISCUSSION

The solvent evaporation method used to make solidifying microspheres and the rate at which the solvent is removed affect how the microspheres appears. In this study, the heating rate of the system was increased to control how fast the solvent evaporated and how it was reflected in its properties. Different variables have been studied, and based on the experimental design, it was found that all the dependent variables depend on the chosen independent variables and vary a lot between the 3 batches (F1 to F3)<sup>58</sup>. At 40 °C, solvent removal is fast and, as a result, the droplets were subjected to stirrer shear pressures prior to solidification for a shorter period. Consequently, in the primary emulsion, the droplet size distribution reflects the microspheres' size dissemination in the wake of joining both emulsion phases. The increased coalescence with higher preparation temperatures was the primary cause of the microspheres' increased size. It is in this light that the unusually wide molecular dispersion in these circumstances can be justified. However, at a lower temperature, 10 °C concentrated emulsification is more likely to occur, resulting in little beads with a uniform size distribution<sup>11,13,59</sup>. Due to the influence of emulsion stabilizer incorporation, the temperature had a moderate effect on the microencapsulation efficiency. The overall fabrication

process's net solvent removal rate from microspheres and the production of microsphere shells caused the microsphere's diameter to shrink because of solvents diffusing out through the trunk of the microsphere. The quick hardening of polymers, which leads to a denser outer layer, has been said repeatedly to make loading more effective. Many things can cause the polymer to solidify quickly, such as a higher solvent removal rate, a higher polymer concentration, or a lower dispersed phase to continuous phase ratio. Drug encapsulation should work well because microspheres made at high temperatures (like 40 °C) quickly harden and form a thin, dense skin. In summary, solvent elimination happens quickly, and microspheres harden practically instantly at high temperatures. Consequently, high-temperature-produced microspheres have a lower density, a porous interior structure, a larger mean size, and a wider size distribution<sup>11,59</sup>. The effect of temperature on molecule shape can also be explained by the rate of solvent expulsion and variation in the continuous form. It may be due to microspheres isolated from liquid paraffin at 10 °C because the dispersion was so sticky. High viscosity is also the cause of the unorthodox configuration of the microspheres formed at 10 °C. Considering the slower elimination of solvent from the inward phase, the polymer solution (droplets) changes gradually into an increasingly thicker stage, where a droplet is entirely vulnerable to mechanical strain. At the point when the mixing paddle hits the emulsion bead, it distorts it, but a sporadic shape normally rapidly changes into a thermodynamically ideal circular shape. Nevertheless, when the viscosity is high, the process is slow, and solidification may occur while the highly viscous droplet is deformed. As a result, microspheres are hardening in an unusual pattern<sup>11,12</sup>. The FTIR data showed that the positions of the different absorption bands and the bonds of the different functional groups in the medicament made at different temperatures did not change. These results strongly suggest that the drug doesn't change much from its original form during the preparation process and that the drug and excipients don't interact during the encapsulation process<sup>60,61</sup>. Due to their small size and uneven, rough, and wrinkled surfaces, which gave them a large surface area for faster DR, DR from microspheres made at a lower temperature was faster than that from microspheres made at a higher temperature. This conclusion fits with the general rule, which is that microspheres' small size gives them a large surface area as well as lesser thickness for faster DR<sup>59,61,62</sup>. By looking at all the release kinetics, or the pattern of drug release, the process of diffusion can be seen<sup>56,63,64</sup>.

## CONCLUSION

Utilizing the solvent evaporation technique, effective indinavir sulfate microspheres were formulated. All formulations' yield and entrapment efficiency were excellent. Resolution of the effects of the preparation temperature on a few characteristics and indinavir release profiles of ethylcellulose microspheres, as well as how the sphericity of the microspheres was affected. The mean particle size of the microspheres was seen to rise at high preparation temperatures because of quick solvent evaporation and an extension of the dissolution time. The sluggish creation of microspheres with a rough surface and structure at low preparation temperatures, however, resulted in a decrease in the mean particle size of microspheres, which decreased the dissolution time. It has been discovered that microspheres created at room temperature have the ideal particle size. The obtained results indicate that preparation temperature greatly influences microsphere formation, resulting in differences in their structure (size and shape), solvent removal rate, and encapsulation efficiency, which in turn alter the overall release patterns of the microspheres. It was determined through the evaluation of the release kinetics that the DR from ethylcellulose microspheres complied with zero-order. A steady release mechanism was suggested for the DR of microspheres.

## ACKNOWLEDGEMENT

Authors thank the Indian Institute of Technology, Kharagpur, for the SEM studies and everyone else who helped to finish this project.

## REFERENCES

1. De Britto D. De Moura M. R. Aouada F. A. Pinola F. G. Lundstedt L. M. Assis O. B. G. and Mattoso L. H.: Entrapment characteristics of hydrosoluble vitamins loaded into chitosan and N, N, N-trimethyl chitosan nanoparticles, **Macromol. Res.**, 2014, 22, 1261-1267.
2. Marimuthu M. Bennet D. and Kim S.: Self-assembled nanoparticles of PLGA-conjugated glucosamine as a sustained transdermal drug delivery vehicle, **Polym. J.**, 2013, 45(2), 202-209.
3. El-Say K. M. El-Helw A. R. M. Ahmed O. A. Hosny K. M. Ahmed T. A. Kharshoum R. M. Fahmy U. A. and Alsawahli M.: Statistical optimization of controlled release microspheres containing cetirizine hydrochloride as a model for water soluble drugs, **Pharm. Dev. Technol.**, 2015, 20(6), 738-746.
4. Sullad A. G. Manjeshwar L. S. and Aminabhavi T. M.: Blend microspheres of chitosan and polyurethane for controlled release of water-soluble antihypertensive drugs, **Polym. Bull.**, 2015, 72, 265-280.
5. Priya Dasan K. and Rekha C.: Polymer blend microspheres for controlled drug release: the techniques for preparation and characterization: a review article, **Curr. Drug. Deliv.**, 2012, 9(6), 588-595.
6. Wang Q. Fu A. Li H. Liu J. Guo P. Zhao X. S. and Xia L. H.: Preparation of cellulose-based microspheres by combining spray coagulating with spray drying, **Carbohydr. Polym.**, 2014, 111, 393-399.
7. Meeus J. Lenaerts M. Scurr D. J. Amssoms K. Davies M. C. Roberts C. J. and Van den Mooter G.: The influence of spray-drying parameters on phase behavior, drug distribution, and *in vitro* release of injectable microspheres for sustained release, **J. Pharm. Sci.**, 2015, 104(4), 1451-1460.
8. Wu J. H., Wang X. J., Li S. J., Ying X. Y., Hu J. B., Xu X. L., Kang X. Q., You J. and Du Y. Z.: Preparation of ethyl cellulose microspheres for sustained release of sodium bicarbonate, **Iran. J. Pharm. Res.**, 2019, 18(2), 556-568.
9. Choi J. W., Park J. H., Baek S. Y., Kim D. D., Kim H. C. and Cho H. J.: Doxorubicin-loaded poly (lactic-co-glycolic acid) microspheres prepared using the solid-in-oil-in-water method for the transarterial chemoembolization of a liver tumor, **Colloids Surf. B. Biointerfaces**, 2015, 132, 305-312.
10. Wang Y., Molin D. G., Sevrin C., Grandfils C., Vanden Akker N. M., Gagliardi M., Knetsch M. L., Delhaas T. and Koole L. H.: *In vitro* and *in vivo* evaluation of drug-eluting microspheres designed for transarterial chemoembolization therapy, **Int. J. Pharm.**, 2016, 503(1-2), 150-162.
11. Yang Y. Y., Chia H. H. and Chung T. S.: Effect of preparation temperature on the characteristics and release profiles of PLGA microspheres containing protein fabricated by double-emulsion solvent extraction/evaporation method, **J. Control. Release**, 2000, 69(1), 81-96.
12. Miyazaki Y., Onuki Y., Yakou S. and Takayama K.: Effect of temperature-increase rate on drug release characteristics of dextran microspheres prepared by emulsion solvent evaporation process, **Int. J. Pharm.**, 2006, 324(2), 144-151.
13. Matević-Rojnik T., Frlan R., Bogataj M., Bukovec P. and Mrhar A.: Effect of preparation temperature in solvent evaporation process on Eudragit RS microsphere properties, **Chem. Pharm. Bull.**, 2005, 53(1), 143-146.
14. Chung T. W., Huang Y. Y. and Liu Y. Z.: Effect of the rate of solvent evaporation on the characteristics of drug loaded PLLA and PDLLA microspheres, **Int. J. Pharm.**, 2001, 212(2), 161-169.
15. Sato T., Kanke M., Schroeder H. G. and Deluca P. P.: Porous biodegradable microspheres for controlled drug delivery. I. Assessment of processing conditions and solvent removal techniques, **Pharm. Res.**, 1988, 5(1), 21-30.
16. Bogataj M., Mrhar A., Kristl A. and Kozjek F.: Eudragit microspheres containing bacampicillin: Preparation by solvent removal method, **J. Microencapsul.**, 1991, 8(3), 401-406.
17. Wang J. and Schwendeman S. P.: Mechanism of solvent evaporation encapsulation process: Prediction of solvent evaporation rate, **J. Pharm. Sci.**, 1999, 88(10), 1090-1099.



18. Sahoo S. K., Dhal S., Mohapatra P., Behera B. C. and Barik B. B.: Effect of processing temperature on Eudragit RS PO microsphere characteristics in the solvent evaporation process, **Pharmazie**, 2007, 62(8), 638-639.
19. Gabor F., Ertl B., Wirth M. and Mallinger R.: Ketoprofen poly (D, L-Lactic-coglycolic acid) microspheres: Influencing of manufacturing parameters and type of polymer on the release characteristics, **J. Microencapsul.**, 1999, 16(1), 1-12.
20. Ly J. and Wu W. Y.: Bimodal release of theophylline from seed-matrix beads made of acrylic polymers, **Pharm. Dev. Technol.**, 1999, 4(2), 257-267.
21. Legrand J., Brujest L., Garnellet G. and Phalip P.: Study of a microencapsulation process of a virucide agent by a solvent evaporation technique, **J. Microencapsul.**, 1995, 12(6), 639-649.
22. Mateovic T., Kriznar B., Bogataj M. and Mrhar A.: The influence of stirring rate on biopharmaceutical properties of Eudragit RS microspheres, **J. Microencapsul.**, 2002, 19(1), 29-36.
23. Bodmeier R. and McGinity J. W.: Solvent selection in the preparation of poly (DL lactide) microspheres prepared by the solvent evaporation method, **Int. J. Pharm.**, 1988, 43(1-2), 179-186.
24. Sansdrap P. and Moes A. J.: Influence of manufacturing parameters on the size characteristics and the release profiles of nifedipine from poly (DL-lactide-co-glycolide) microspheres, **Int. J. Pharm.**, 1993, 98(1-3), 157-164.
25. Leach K., Noh K. and Mathiowitz E.: Effect of manufacturing conditions on the formation of double walled polymer microspheres, **J. Microencapsul.**, 1999, 16(2), 153-167.
26. Bogataj M., Mrhar A., Grabnar I., Rajtman Z., Bukovec P., Srcic S. and Urleb U.: The influence of magnesium stearate on the characteristics of mucoadhesive microspheres, **J. Microencapsul.**, 2000, 17(4), 499-508.
27. Du W., Wu P., Zhao Z. and Zhang X.: Facile preparation and characterization of temperature-responsive hydrophilic crosslinked polymer microspheres by aqueous dispersion polymerization, **Eur. Polym. J.**, 2020, 128, 109610.
28. Yasin H., Al-Taani B. and Salem M.S.: Preparation and characterization of ethylcellulose microspheres for sustained-release of pregabalin, **Res. Pharm. Sci.**, 2021, 16(1), 1-15.
29. Iordache T. V., Banu N. D., Giol E. D., Vuluga D. M., Jerca F. A. and Jerca V. V.: Factorial design optimization of polystyrene microspheres obtained by aqueous dispersion polymerization in the presence of poly (2-ethyl-2-oxazoline) reactive stabilizer, **Polym. Int.**, 2020, 69(11), 1122-1129.
30. Jain P., Garg A., Farooq U., Panda A. K., Mirza M. A., Noureideen A., Darwish H. and Iqbal Z.: Preparation and quality by design assisted (Qb-d) optimization of bioceramic loaded microspheres for periodontal delivery of doxycycline hyclate, **Saudi. J. Biol. Sci.**, 2021, 28(5), 2677-2685.
31. Mulla T. S., Salunkhe V. R., Bhinge S. D. and Mohire N.: Formulation, design and optimization of antidiabetic drug loaded microspheres, **Polym. Bull.**, 2022, 7, 1-26.
32. Mwila C. and Walker R.B.: Improved stability of rifampicin in the presence of gastric-resistant isoniazid microspheres in acidic media, **Pharmaceutics**, 2020, 12(3), 234.
33. Mali A., Mali S. and Bathe R.: Design, characterization and evaluation of tramadol HCL loaded microsphere prepared by emulsion solvent evaporation method, **J. Adv. Sci. Res.**, 2020, 11(04), 262-267.
34. Obaidat R., Al-Ghzawi B., Al-Taani B. and Al-Shar'i N.: Co-crystallization of amoxicillin trihydrate and potassium clavulanate provides a promising approach for preparation of sustained-release microspheres, **AAPS. Pharm. Sci. Tech.**, 2022, 23(5), 131.
35. Panda S., Sahu A., Mohanty B. R., Nayak B. S. and Mishra B.: Formulation and *in vitro* characterization of lamivudine embedded natural resin microspheres using olibanum as drug carriers, **Res. J. Pharm. Life. Sci.**, 2020, 1(2), 83-102.
36. Pignatello R., Pecora T. M., Cutuli G. G., Catalfo A., De Guidi G., Ruozi B., Tosi G., Cianciolo S. and Musumeci T.: Antioxidant activity and photostability assessment of trans-resveratrol acrylate microspheres, **Pharm. Dev. Technol.**, 2019, 24(2), 222-234.
37. Malvey S., Muthu A. K., Balamurugan K., Rao J. V., Puchchakayala G., Ravinder E. and Kshirasagar N.: Mucoadhesive Microsphere Drug Delivery System (MMDDS): A Mini Review, **Int. J. Clin. Exp. Med. Res.**, 2021, 5(4), 435-444.
38. Li P., Qin L., Wang T., Dai L., Li H., Jiang J., Zhou J., Li H., Cheng X. and Lei F.: Preparation and adsorption characteristics of rosin-based polymer microspheres for berberine hydrochloride and separation of total alkaloids from *Coptidis rhizoma*, **Chem. Eng. J.**, 2020, 392, 123707.
39. Natarajan R., Venkataraman S., Rajendran D. S., Tamilselvam B., Zaveri H., Jeyachandran N., Prashar H. and Vaidyanathan V. K.: Adsorption performance of magnetic mesoporous silica microsphere support toward the remediation of acetaminophen from aqueous solution, **J. Water. Process. Eng.**, 2022, 48, 102835.
40. Faidi A., Lassoued M. A., Becheikh M. E., Touati M., Stumbé J. F. and Farhat F.: Application of sodium alginate extracted from a Tunisian brown algae *Padina pavonica* for essential oil encapsulation: Microspheres preparation, characterization and *in vitro* release study, **Int. J. Biol. Macromol.**, 2019, 136, 386-394.
41. Pandey N., Sah Dr. A. N. and Mahara K.: Formulation and evaluation of floating microspheres of nateglinide, **Int. J. Pharm. Sci. Res.**, 2016, 7(11), 453-464.
42. Uyen N. T., Hamid Z. A., Tram N. X. and Ahmad N.: Fabrication of alginate microspheres for drug delivery: A review, **Int. J. Biol. Macromol.**, 2020, 153, 1035-1046.
43. Wang J., Helder L., Shao J., Jansen J. A., Yang M. and Yang F.: Encapsulation and release of doxycycline from electrospray generated PLGA microspheres: Effect of polymer end groups, **Int. J. Pharm.**, 2019, 564, 1-9.
44. Agrawal G. R., Wakte P., and Shelke S.: Formulation, physicochemical characterization and *in vitro* evaluation of human insulin-loaded microspheres as potential oral carrier, **Prog. Biomater.**, 2017, 6(3), 125-136.



45. Lee J. and Sah H.: Preparation of PLGA nanoparticles by milling spongelike PLGA microspheres, **Pharmaceutics**, 2022, 14(8), 1540.
46. Ramanathan G., Thyagarajan S. and Sivagnanam U. T.: Accelerated wound healing and its promoting effects of biomimetic collagen matrices with siderophore loaded gelatin microspheres in tissue engineering, **Mater. Sci. Eng. C. Mater. Biol. Appl.**, 2018, 93, 455-464.
47. Liu H., Zhai X., Li Z., Tao X., Gao S., Zhao J. and Liu W.: Effect of mesoporous  $\alpha$ -Fe<sub>2</sub>O<sub>3</sub> nanoparticles doping on the structure and electrochemical hydrogen storage properties of Co<sub>0</sub>. 9Cu<sub>0</sub>. 1Si alloy, **J. Alloys Compd.**, 2018, 755, 147-153.
48. Ahmed M. M.: Effect of different formulation variables on release characteristics of gastro-floating microspheres of ethyl cellulose/carbopol 934P encapsulating sorafenib, **Int. J. Pharm. Pharm. Sci.**, 2019, 11(10), 64-70.
49. Aydogan E., Comoglu T., Pehlivanoglu B., Dogan M., Comoglu S., Dogan A. and Basci N.: Process and formulation variables of pregabalin microspheres prepared by w/o/o double emulsion solvent diffusion method and their clinical application by animal modeling studies, **Drug. Dev. Ind. Pharm.**, 2015, 41(8), 1311-1320.
50. Shekar H. S., Rajamma A. J. and Sateesha S. B.: Ultrasound induced microencapsulation of simvastatin for gastric retention and controlled delivery, **Indian. J. Pharm. Sci.**, 2018, 80(4), 647-656.
51. Momoh M. A., Jackson T. C., Musiliu A. O., Chimaobi K. F., Darlington Y. C. and Ofokansi K.C.: Microspheres of insulin-Eudragit complex: Formulation, characterization and *in vivo* studies, **Afr. J. Pharm. Pharmacol.**, 2017, 11(29), 327-341.
52. Saxena A. and Kitawat S.: Formulation, Development and evaluation of microspheres of ketoprofen by using different polymers, **ASIO. J. Pharm. Herb. Med. Res.**, 2015, 1(1), 41-47.
53. Gupta V., Singh S., Srivastava M., Ahmad H., Pachauri S. D., Khandelwal K., Dwivedi P. and Dwivedi A. K.: Preparation and characterization of depot injectable microspheres of centchroman using ethyl cellulose, **J. Biomater. Tissue Eng.**, 2014, 4(4), 259-268.
54. Shukla R., Gupta J., Shukla P., Dwivedi P., Tripathi P., Bhattacharya S. M. and Mishra P. R.: Chitosan coated alginate micro particles for the oral delivery of antifilarial drugs and combinations for intervention in *Brugia malayi* induced lymphatic filariasis, **RSC. Adv.**, 2015, 5(85), 69047-69056.
55. Hajare P. P. and Rachh P. R.: Gastroretentive microballoons: a novel approach for drug delivery, **Int. J. Pharm. Sci. Res.**, 2020, 11(3), 1075-1083.
56. Siepmann J. and Siepmann F.: Mathematical modeling of drug delivery, **Int. J. Pharm.**, 2008, 364(2), 328-343.
57. Siepmann J. and Peppas N. A.: Mathematical modeling of controlled drug delivery, **Adv. Drug. Deliv. Rev.**, 2001, 48(2-3), 137-138.
58. Dey S., Pramanik S. and Malgope A.: Formulation and optimization of sustained release stavudine microspheres using response surface methodology, **ISRN. Pharm.**, 2011, 1-7.
59. Heiskanen H., Denifl P., Pitkänen P. and Hurme M.: Effect of concentration and temperature on the properties of the microspheres prepared using an emulsion solvent extraction process, **Adv. Powder. Technol.**, 2012, 23(6), 779-786.
60. Li L., Yang Y., Lv Y., Yin P. and Lei T.: Porous calcite CaCO<sub>3</sub> microspheres: Preparation, characterization and release behavior as doxorubicin carrier, **Colloid Surf. B. Biointerfaces**, 2020, 186, 110720.
61. Luo C., Yang Q., Lin X., Qi C. and Li G.: Preparation and drug release property of tanshinone IIA loaded chitosan-montmorillonite microspheres, **Int. J. Biol. Macromol.**, 2019, 125, 721-729.
62. Chowdary K. P. R., Rao N. K. and Malathi K.: Ethyl cellulose microspheres of glipizide: Characterization *in vitro* and *in vivo* evaluation, **Indian J. Pharm Sci.**, 2004, 66(4), 412-416.
63. Ramteke K. H., Dighe P. A., Kharat A. R. and Patil S. V.: Mathematical models of drug dissolution: a review, **Sch. Acad. J. Pharm.**, 2014, 3(5), 388-396.
64. Siepmann J. and Peppas N. A.: Modeling of drug release from delivery systems based on hydroxypropyl methylcellulose (HPMC), **Adv. Drug. Deliv. Rev.**, 2012, 64, 163-174.

**For Advertising in the Classified Columns and also for series advertisements please contact: Geeta Suvarna (+9820161419)  
Publications Department**



## **IDMA BULLETIN**

Tel.: 022 - 2494 4624 / 2497 4308 E-mail: [publications@idmaindia.com](mailto:publications@idmaindia.com)  
Website: [www.idma-assn.org](http://www.idma-assn.org), [www.indiandrugsonline.org](http://www.indiandrugsonline.org)